water

MDPI

Article

Spatial and Temporal Effects of Irrigation Canals Rehabilitation on the Land and Crop Yields, a Case Study: The Nile Delta, Egypt

Sherien Abd-Elziz [1], Martina Zeleňáková [2,*], Branislav Kršák [3] and Hany F. Abd-Elhamid [4,5]

[1] Ministry of Water Resources & Irrigation, Imbaba, Giza 12666, Egypt; sherien.abdelaziz@eng.zu.edu.eg
[2] Department of Environmental Engineering, Faculty of Civil Engineering, Technical University of Kosice, Vysokoškolská 4, 040 01 Košice, Slovakia
[3] Institute of Earth Resources, Faculty of Mining, Ecology, Process Control and Geotechnologies, Technical University of Kosice, Vysokoškolská 4, 040 01 Košice, Slovakia; branislav.krsak@tuke.sk
[4] Department of Water and Water Structures Engineering, Faculty of Engineering, Zagazig University, Zagazig 44519, Egypt; hany_farhat2003@yahoo.com
[5] Center for Research and Innovation in Construction, Faculty of Civil Engineering, Technical University of Kosice, 040 01 Košice, Slovakia
* Correspondence: martina.zelenakova@tuke.sk; Tel.: +421-55-602-4270

Abstract: Shortage of surface water is considered an international problem that has even extended to countries that have rivers, in particular countries sharing the same river basins and downstream countries, such as Egypt. This issue requires intensive management of available water resources. Irrigation Canals Rehabilitation (ICR) has become essential to protect surface water in irrigation canals from losses due to seepage. Egypt is one of the countries that has started using this technique. This paper aims to evaluate the impact of ICR using concrete on the land and on crop yields. The SEEP/W model is used in the current study to estimate changes in the groundwater table and moisture in the root zone. Three cases studies have been simulated and compared including unlined, lined, and lined canals with a drainage pipe. The methodology is applied to three canals in the Nile Delta: Sero, Dafan, and New-Aslogy. The results demonstrate that ICR has decreased the losses from canals which resulted in lowering the groundwater, where the case of lining gave a higher reduction than the case of lining with a drainage pipe. In addition, the water table underneath the embankment was lowered. Decreasing the groundwater table could help to protect the land from logging and increase crop yields, but it may reduce the recharging of groundwater aquifers. Such a study is highly recommended in arid regions to decrease water losses where many countries are suffering from water shortage.

Keywords: irrigation canals rehabilitation; seepage; crop yields; embankment; side slope; Nile Delta

check for updates

Citation: Abd-Elziz, S.; Zeleňáková, M.; Kršák, B.; Abd-Elhamid, H.F. Spatial and Temporal Effects of Irrigation Canals Rehabilitation on the Land and Crop Yields, a Case Study: The Nile Delta, Egypt. *Water* **2022**, *14*, 808. https://doi.org/10.3390/w14050808

Academic Editor: Guido D'Urso

Received: 16 January 2022
Accepted: 28 February 2022
Published: 4 March 2022

Publisher's Note: MDPI stays neutral with regard to jurisdictional claims in published maps and institutional affiliations.

Copyright: © 2022 by the authors. Licensee MDPI, Basel, Switzerland. This article is an open access article distributed under the terms and conditions of the Creative Commons Attribution (CC BY) license (https://creativecommons.org/licenses/by/4.0/).

1. Introduction

Canals are used to deliver surface water from the source to the end user. They may be used to supply water to many sectors, including the agricultural, industrial, and domestic sectors. Multiple efforts are made to maintain the function of canals delivering water to all outlets, as well as to the ends of canals. Zeng et al. [1] optimized the control of cascaded irrigation canals by controlling the minimum water levels required for irrigation and preventing dam collapse as a result of water overflows using control gates and interconnected long-distance reaches. Rath and Swain [2] evaluated the performance of the Hirakud canal system in Odisha, India. The flow was measured by an ADV flow tracker. The performance of the canals was assessed through variability, adequacy, inequity, efficiency, conveyance performance, and irrigation performance, which showed that the strategy of canal operation should be interested in obtaining an optimal yield. Controlling the seepage from canals to the groundwater under the canal bed or to the groundwater in

the neighboring lands has become a goal everywhere to save surface water. Zhou et al. [3] developed an uncomplicated procedure to evaluate water consumption and return flow in the period from 1980 to 2010 at four hot-spot irrigated areas on the field and regional scales. The results demonstrated a decrease in evaporated water. For the regional scale, water leached to the aquifers was classified as advantageous rather than waste. Khanal et al. [4] analyzed factors affecting irrigation water users collective action for managing their uses in an irrigation system by the year 2019 through applying a simple random sampling method for cross-sectional data from 184 points. Data analysis utilized a logit regression method. The collective action for managing the irrigation water system was changed by a combination of various factors: the age of the household head, his level of schooling, the presence of monetary fines and the number of farmers in a branch of the irrigation system.

Morad and Abdel Latif [5] reported that 95% of total groundwater recharge was due to seepage from a canal and 5% from percolation in the study area between Borg El Arab and El Hammam, Egypt. Awad and El Fakharany [6] used MODFLOW and MODPATH models to ensure that the problem of water logging was due to seepage from the Ismailia canal and the irrigation network, in addition to excess irrigation water. Rank and Vishnu [7] evaluated the features of noncontinuous irrigation, which helps the crop root zone in better growth of the plant by allowing aeration of the root zone. Air is essential to the plant in the photosynthesis process. Thus, this process could increase crop yield. Hosseinzadeh et al. [8] investigated the factors affecting seepage from earthen channels in the Zayandeh-Rud irrigation network, Iran, and the Gediz watershed in Turkey using the finite elements method. The results showed that the wetted perimeter influences seepage from the channels, while the side slope of the channels has only a minor effect. Tavakoli et al. [9] simulated the earthen channel of Boldaji, Borujen city, Chaharmahal and Bakhtiari province, Iran, in the laboratory of Shahrekord University. The results showed that the seepage from the canal increased the groundwater levels by 3.5–11 cm.

A rising water table in the root zone of a plant prevents aeration in the root zone, causing damage to the plant's roots and thus reducing the productivity of cultivated land. This phenomenon, known as land logging, causes heavy economic losses, so there are efforts to lower the groundwater table to more appropriate values. Deng and Bailey [10] analyzed and quantified the cause of high groundwater levels in irrigated stream aquifer systems, in northern Colorado, USA, using global sensitivity analysis (GSA) and a MODFLOW model. The results showed that lining a canal with a sealant to reduce seepage by >50% from surface water irrigation to groundwater irrigation, could lower the groundwater table by 1.5 m to 3 m over a period of five years. The lining of an irrigation canal helps lower the groundwater table and saves surface water as well. Habteyes and Ward [11] developed a state-of-the-art empirical dynamic optimization model to investigate the economic performance of saved water in the Canadian River Basin, southwestern USA. The results proved that the delivery system of a canal lining can raise the sustained economic value of water for crop irrigation, where the saved water can be used in dry years by storing it in wet years.

A fuzzy inference system to control the irrigation system through determining the water irrigation volume for a sweet pepper crop was used by Aquino-Jr et al. [12]. The collected data was used to control the algorithm to ensure that the soil moisture in the root zone was suitable for the plant. Abd-Elaziz et al. [13] mentioned that the minimum depth for groundwater in the root zone ranged from 1.5 m to 0.75 m. Nasr et al. [14] relieved uplift pressure behind the canal lining by locating a tile drain at a position that allowed minimum uplift pressure.

Irrigation Canals Rehabilitation (ICR) is an ideal solution for protecting surface water from percolation into the aquifer, with the saved amount of water used to irrigate reclaimed areas, according to Abuzied et al. [15]. The data used in their research was collected from fields through the official Ministry of Water Resources and Irrigation Authority in Assiut governorate, Egypt. The analysis of the data proved that the total loss of irrigation water

from Almanna canal and its branches reaches about 16.05 million m^3 monthly. The water lost through only seepage reaches about 15.95 million m^3 monthly, representing 99% of all lost irrigation water. Shah et al. [16] used the inflow–outflow method for seven concrete-lined distributary canals in Punjab, Pakistan, then compared his results with results from five empirical formulae. The comparison showed that the mean percent errors ranged from −20% to +19%. Han et al. [17] evaluated the seepage from canals by monitoring water levels using different lining materials under different service times. The results showed that cracks in the joints between the precast concrete slabs and holes in the geomembrane were the reason for the seepage loss, while lining reduced seepage by 86% compared to there being no lining. Eltarabily et al. [18] determined the effect of canal-lining on groundwater levels using MODFLOW to simulate the interaction between surface and groundwater for the Ismailia canal, Egypt. This estimated the seepage from the unlined canal to the aquifer to be at 3.5 million m^3/day, which represents 21.6% of the canal's total discharge. Abd-Elhamid et al. [19] proved that lessening the conductivity of lining materials decreased the contamination from an open drain into the groundwater. This reduction reached 43%, 89.6%, 91.4%, and 93% using several lining materials, such as geomembranes, clay, concrete, and bentonite.

Khan et al. [20] observed a gradual rise in electrical conductivity (EC), using Visual MODFLOW to simulate the effects of a concrete lining on groundwater. Lesser et al. [21] determined the effect of lining canals on groundwater levels in the Mexicali Valley. The groundwater flow model recorded a remarkable drawdown after the lining was added in 2008, where the water table dropped to 5.8 m at the end of four years of monitoring. Zhao et al. [22] adopted a methodology for estimating the spatial and temporal extensive soil moisture datasets in the Shale Hills Critical Zone Observatory (CZO), China, in the period from 2004 to 2010. The methodology used an Empirical Orthogonal Function (EOF) analysis to evaluate the soil moisture. In addition, Taran and Mahtabi [23] investigated the effect of three weep holes on managing the uplift pressure under concrete-lined canals under the condition of fluctuating groundwater levels. The discharge was measured from these weep holes in the physical model. Another simulation using a SEEP/W numerical model was performed to measure the discharge. The results indicated that uplift pressure values were under the condition of fluctuating groundwater levels, and the maximum hydraulic gradient occurred at the corner of the canal bed. Salmasi et al. [24] investigated a drainage system (drain pipes under the canal bed) to reduce uplift forces and to increase canal stability against fluctuating groundwater levels.

Taran and Mahtabi [23] also investigated the effect of three weep holes on managing the uplift pressure under concrete-lined canals under the condition of fluctuating groundwater levels. The discharge was measured from these weep holes in the physical model. Another simulation using a SEEP/W numerical model was performed to measure the discharge. The results indicated that uplift pressure values were under the condition of fluctuating groundwater levels, and the maximum hydraulic gradient occurred at the corner of the canal bed. Salmasi et al. [24] investigated a drainage system (drain pipes under the canal bed) to reduce uplift forces and to increase canal stability against groundwater fluctuated levels.

In the context of the pressing need for water as a result of growth of population, projects made by upper stream countries such as the Grand Ethiopian Renaissance Dam (GERD), and severe climate change, Egypt takes serious steps respected by the international community to reduce the risks of the increased shortage in water resources through reducing its birth rate and continuous negotiation with the Ethiopians. Egypt realizes the risks which are a threat to the planet due to climate changes. Egypt participated and supported the decisions taken by an international conference held by Ministry of Water Resources and Irrigation (MWRI) in October 2021 under ascendancy of the climate changes. Egypt managed its resources and applied an urgent policy of Irrigation Canals Rehabilitation (ICR) to restore canal cross-sections to their designed section and reduce seepage from

canal boundaries into groundwater [25]. The rehabilitation of canals is done through a concrete lining.

This study aims to estimate the effect of ICR on the seepage from canals by presenting the alteration in the groundwater table before and after the lining process for different locations at different times until reaching a steady state condition. The simulation was performed for steady/unsteady conditions. It is important to estimate the suitability of the new groundwater table for the vadose zone of plants through detection of pore water pressure and by comparing among three states: the canal before the lining (unlined state), the lined case, and the lined case with a drainage pipe. Flux was estimated for the three cases to evaluate the changes in seepage through the downstream embankment (the embankment toe) to measure the role of the lining in reducing conductance between the embankment and the other parts of the aquitard. The simulation was performed using a SEEP/W model to compute heads, flux, pore water pressure, and the water table for the selected cases.

2. Materials and Methods

2.1. The Study Area

Egypt has a hierarchy system for its irrigation canals. The top of the hierarchy system is the Nile River which is the main source of water in Egypt. In the hierarchy system, the Nile River is followed by Rayah, which in turn supplies the main canals. The main canal supplies branch canals, and the destination is meska or marwa (a very small canal used in irrigation in farms) [26].

A pilot study area representing the Nile Delta boundary conditions was selected in the Sharkia Governorate. The city of Zagazig is the capital of the Sharkia Governorate and is located 70 km north-east of Cairo (the capital of Egypt). Three canals were selected from the irrigation network of the Sharkia Governorate to perform the current study; these were the Sero, Dafan, and New-Aslogy canals. Each one of them belongs to a different zone, as indicated in Figure 1a. The first canal, Sero, is located in the Abu Kabir zone (Figure 1b); the second canal, New-Aslogy, is located in the Zagazig zone (Figure 1c); and the third canal, Dafan, is located in the Awlad-sakr zone (Figure 1d). Table 1 shows the main data for the selected canals.

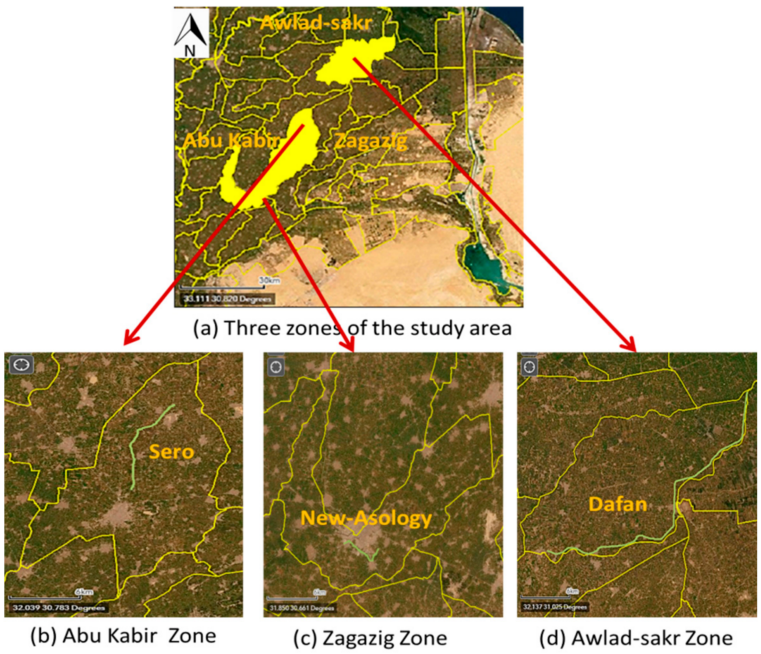

Figure 1. Location map of the study area [27].

Table 1. Main data of the selected canals.

The Canal	Length (km)	Zone	Pick Point	Longitude	Latitude
Sero	11.155	Abu Kabir	end	31.721°	30.835°
Dafan	36.899	Awlad-sakr	inlet	31.706°	30.931°
New-Aslogy	6.187	Zagazig	inlet	31.482°	30.576°

2.1.1. Surface Water System in the Study Area

The surface system includes the irrigation network, which is a part of the hierarchy system of Egypt that is considered the surface water source in the pilot areas, given the small, fluctuating amount of precipitation in this arid zone. The climate is hot, dry, and rainless in summer, and it is mild with little rain in winter. The average annual rainfall is estimated to be 51 mm/year. The mean daily temperature is 12 °C during the winter and rises to 37 °C in the summer.

2.1.2. Groundwater System in the Study Area

The pilot area is a part of the Nile Delta aquifer system, which is defined as a semi-confined aquifer. The upper layer is leaky and semi-permeable, formed from Holocene silt and clay with a thickness differing from 0 to 20 m, which is called the aquitard or clay cap and is the layer of interest in this study [13]. Table 2 provides the examined depths for each studied location, as extracted from reports on soil samples at these locations in the years 2018 and 2019 [28]. The middle layer is the aquifer, which consists of sand and gravel with clay lenses [13]. The lower layer is Pliocene marine clay (the impermeable boundary), which is known as the aquiclude (sticky clay).

Table 2. Geometric data of the selected canals.

Canal	Section (km)	Side Slope	Surface Water Level	Ground-Water Level	Bed Width (m)	Bed Level	Road Width (m)	Road Level	Aquitard Depth (m)
Sero	1.00	1:1	(5.50)	(1.90)	6	(2.70)	12	(5.70)	12.5
	7.00		(4.50)		5	(1.90)	7.4	(5.00)	
	10.55		(4.40)		4	(1.90)	4.9	(5.00)	
Dafan	17.500	1:1	(0.40)	−(0.75)	8	−(1.30)	5.5	(2.75)	9.3
New-Aslogy	1.500	1:1	(8.84)	(5.94)	3	(6.90)	6.57	(9.33)	9.2

The aquitard properties required for the simulation were saturated hydraulic conductivity in the x-direction (k_x), saturated water content (swc)%, residual water content, and the coefficient of volume compressibility (m_v). Hydraulic conductivity controls the seepage in both directions and is 0.2 m/day; the anisotropy ratio K_y/K_x is one, where the aquitard is isotropic; and swc expresses the maximum amount of water that the soil can store. It strongly related to the clay porosity; the value in the simulation was 0.38%, while the coefficient of volume compressibility was 0.075×10^{-3} kpa. The residual water content refers to the water content of the soil where a further increase in negative pore-water pressure does not produce significant changes in the water content; here the value of 0.068 was used in the simulation, while the porosity of the lining material is 10–35% [29].

2.1.3. Interaction between the Surface and Groundwater Systems and Discharge in the Study Area

The interaction between the surface water and groundwater systems in the pilot areas is represented in the natural recharging of the aquifer via three directions: 1. infiltration from the irrigation canals network to the shallow aquifer or the clay cap, 2. excess water in the root zone flowing under gravity and capillary fringes to the aquifer under the

cultivated area in the vadose zone, and 3. the loss of surface water to the shallow aquifer by seepage from the irrigation network to the adjacent lands. This seepage could be useful for maintaining the soil moisture at the desired level of plant needs, but when this amount is exceeded, it causes land logging, crop damage, economic losses etc., so the policy of ICR is considered to be a way to solve the problem of percolation from canals, and ICR is expected to save 6.57 million m^3 of water by the year 2022 [25]. The discharge from the aquifer is the only way to reduce the shortage in supplementary surface water in places where the pilot areas suffer from a severe shortage of surface water, as well as other regions in Egypt. The infiltration from agricultural soil to the canal was taken into consideration in the simulation. Chuck [30] illustrated that the soil texture controls the available water capacity, where clayey soil is within the range 1.20–1.50 inches/foot of depth and the infiltration rate is 0.10–0.20 inches/h. Table 2 shows the geometric data for the Sero, Dafan, and New-Aslogy canals. This data includes the locations of the selected sections to be studied, side slopes, and the surface water levels in the canals; for groundwater, it includes bed widths, bed levels, bank widths and levels, and the depth of the clay cap for each location.

2.2. Numerical Modeling

SEEP/W is a strong finite element software model for simulating groundwater flow in porous media. SEEP/W can simulate simple saturated steady-state difficulties and sophisticated saturated/unsaturated transient conditions. In this regard, it was used to simulate the interaction between surface water in irrigation canals and groundwater in nearby agricultural lands and the aquitard to compute the changes to the groundwater levels due to a concrete lining, which blocks the main source of recharging the shallow aquifer soils. SEEP/W is one of the packages of the Geo-studio program. El-Molla [31] used the SEEP/W model to estimate the impact of a compacted earth lining on seepage from trapezoidal irrigation canals and concluded that a highly compacted earth lining could save 99.8% of the percolated water to the aquifer. Aghdam et al. [32] and Taran and Mahtabi [23] used SEEP/W and showed that drainage pipes could reduce the uplift force for a gravity dam. Salmasi and Abraham [33] and Hosseinzadeh et al. [8] used SEEP/W to predict the seepage from earthen channels at the Zayandeh-Rud irrigation channels, Iran. References [34–37] found that SEEP/W is a good tool to simulate the seepage from surface water to soil and vice versa. The model uses Darcy's Equation, which is expressed as:

$$q = ki \tag{1}$$

where:

1. q: specific discharge (m^3/day/m)
2. k: hydraulic conductivity (m/day)
3. i: gradient of the total hydraulic head (m/m)

The governing differential equation for two-dimensional seepage can be expressed mathematically as SEEP/W [38]:

$$\frac{\partial}{\partial x}\left(kx\frac{\partial H}{\partial x}\right) + \frac{\partial}{\partial y}\left(ky\frac{\partial H}{\partial y}\right) + Q = \frac{\partial \theta}{\partial t} \tag{2}$$

where:

1. H: total head $= h + y$, ie
2. h: pressure head
3. y: elevation
4. kx: hydraulic conductivity in the x-direction
5. ky: hydraulic conductivity in the y-direction
6. Q: applied boundary flux
7. θ: volumetric water content (for clay = 45% to 55%)
8. t: time

While the basic finite element equation is:

$$[k]\{H\} = Q \quad (3)$$

where:

1. k: *element property matrix (includes material properties and volume)*
2. H: nodal total head
3. Q: nodal flow

3. Methodology

The methodological approach used to evaluate the effect of the lining process in keeping surface water from infiltrating into the shallow aquifer was to compare the seepage from unlined canals and concrete-lined canals utilizing SEEP/W; in this way, the suitability of the groundwater level or soil moisture content for the plant root zone after the lining could be estimated.

3.1. Unlined Canals

The data presented in Table 2 was used in the simulation and calibration of the model. Knowing the level of water in the canal and the level of groundwater in the nearby land, the leaching line from the canal to the land, where the water levels in the canals exceeded the groundwater levels for all mentioned sections, could be predicted. For example, the section 1.00 km from the inlet of the Sero canal has a surface water level of (5.20) and a groundwater level of (1.90), so there was continuous seepage moving from the canal to the level of (1.90) in the clay layer. This is not limited to this section; all unlined canals suffered from seepage into the groundwater. Therefore, there was a loss in surface water due to seepage from canals, meaning there is a need to apply ICR. The case of unlined canals was one of the three studied cases.

3.2. Lined Canals

The lining would lessen or even fully prevent the seepage into the groundwater aquifer for an optimum lining process, where the permeability of the canal boundaries is limited to the tiniest value due to lining with impermeable materials. A lining material composed of two layers of sandstone pitching with cement mortar with a minimum thickness of 30 cm was applied directly on restored canal boundaries for the designed cross-section. Sandstone has a much higher porosity of 10–35% [39]. The second layer is plain concrete (pc) with a thickness of 10 cm, which is covered with a moisture-insulating material, such as cresol, to fill the pores and block the cracks in the pc layer to prevent percolated water from seeping into the shallow groundwater aquifer. Ref [18] mentioned that canal boundaries lined with concrete possess low permeability, less than 8.64×10^{-5} m/d, while [19] used a value of 4×10^{-9} m/d for the concrete lining. Figure 2 shows a field photo of the Sero canal after lining.

Figure 2. Real photo of the Sero canal after lining.

3.3. Lined Canals with a Drainage Pipe

In some reaches, it was essential to allocate a drainage pipe in the side slope of the canal. The drainage pipe has a diameter of 10 to 15 cm and was placed at a height from 0.75 to 1.5 m above the bed. The function of the drainage pipe is to release groundwater pressure on the side slope of the canal after lining, and its role was to prevent the percolation of this groundwater into the canal when the canal is off or during maintenance periods. In these periods, the level of groundwater exceeded the water levels in the canal. Lined canals had two cases to be studied: lined canals without and lined canals with a drainage pipe.

3.4. Model Geometry and the Grid

Figure 3 gives an example for the simulated canals in the study area. Figure 3a shows the location of the Sero canal, and where it belongs to in the Abo-Kabir zone which appears in green. The 31.682° and 30.749° degrees pick the location of the inlet, while the border of the pilot areas appears in yellow. Figure 3b shows the simulated unlined cross section using SEEP/W, depending on data from the 1.00 km section from Table 2. This description of the section is valid from the inlet to the section at 1.00 km. The applied scale is fine-tuned, using a 1:1 aspect ratio. The mesh consists of 248 nodes and 213 elements, with a default approximate global element size of 1.0 m of quads and triangles, which is the most appropriate, where complexity does not mean an accurate solution.

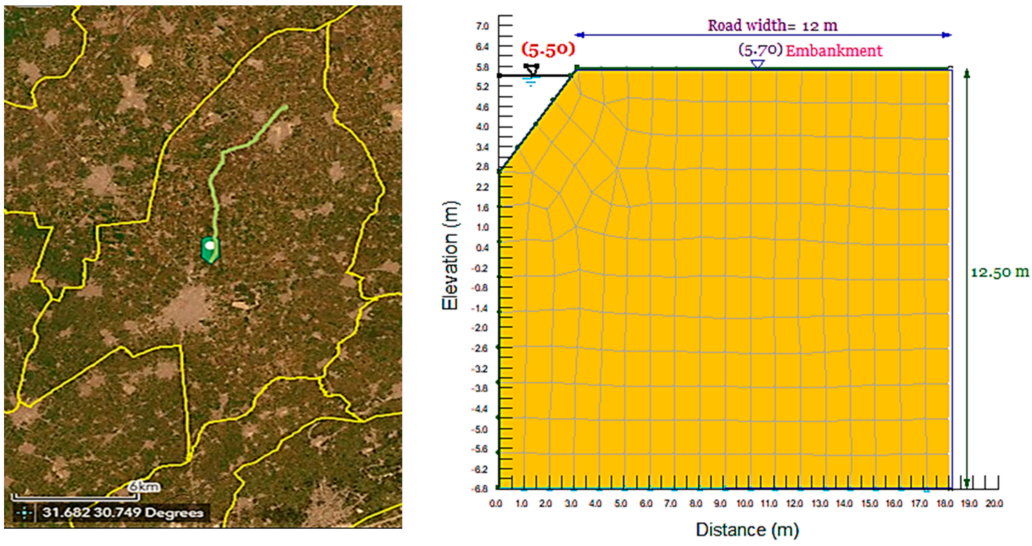

(**a**) The canal location (**b**) The simulation of unlined clayey canal

Figure 3. An example for the simulated canals.

3.5. Properties of Material and Boundary Conditions

Figure 3b indicates that the soil of the embankment is a homogeneous clayey soil, with a width of 12 m and a level of (5.70). The depth of the aquitard is 12.50 m. The bed and surface water levels in the canal are (2.70) and (5.50), respectively. The characteristics of the clay were identified in the simulation. Figure 4 shows the boundary conditions for three cases of the Sero canal: unlined, lined, and lined with a drainage pipe. Figure 4a represents the unlined case; the total head alongside the slope and under the canal is 5.50 and there is a potential seepage face, as shown in the figure downstream from the embankment, to allow seepage to pass through. In Figure 4b, the lining material is in green, the boundary conditions for the lined Sero canal; the total head was only for the side slope of the canal and was 5.50, while the boundary conditions for the side slope of the lined canal were represented by zero head pressure to express the new condition of preventing seepage from the canal. The other condition was a potential seepage face, as shown in the figure. Figure 4c represents the case of the lined canal with a drainage pipe; it has an addition in

the boundary conditions of the lined stated, where the boundary conditions at the drainage pipe are ahead of 5.50 m.

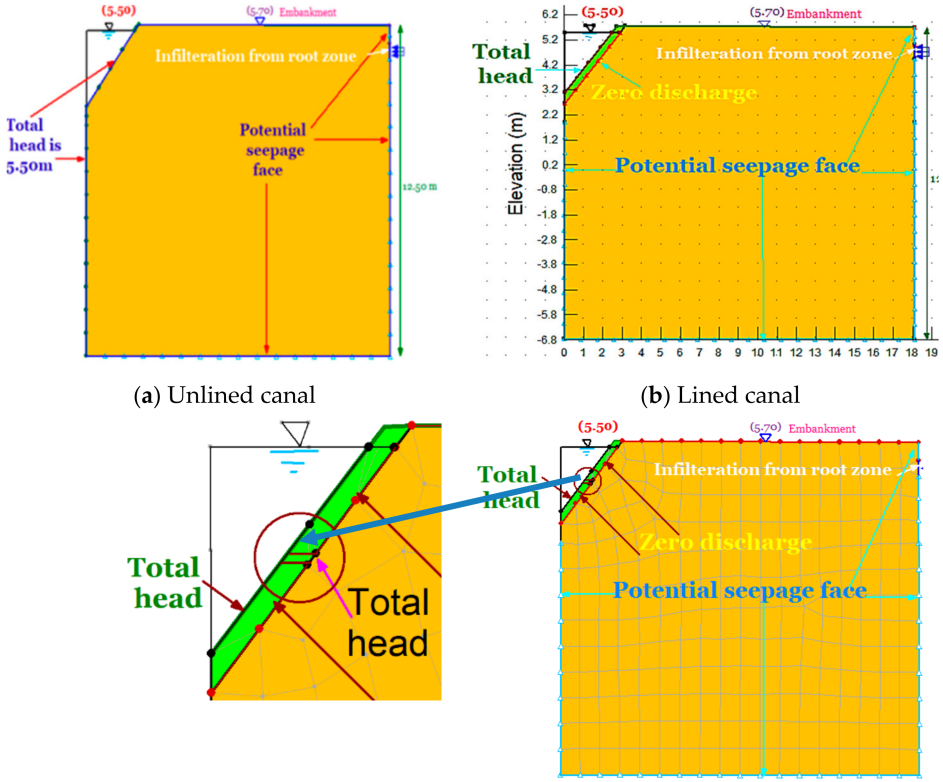

(**a**) Unlined canal (**b**) Lined canal

(**c**) Lined canal with a drainage pipe

Figure 4. Boundary conditions for the Sero canal for three cases.

3.6. Initial Conditions

The proposed cases were simulated for the steady state conditions, especially before the lining, where the canals worked for a long time. A transient analysis was essential to predict the temporal changes alerted to the canals as a reaction to the lining. SEEP/W specified the initial conditions by reading the data from an initial conditions file created in a separate analysis, which called parental analysis (steady state analysis) by defining the initial total head at all nodes created by the steady state analysis. The initial conditions analysis was identical in geometry and material to both simulations. Therefore, the studied cases simulated for transient analysis, particularly for the cases of lining and lining with a drainage pipe depending on a previous simulation (steady state analysis), as follows:

1. Steady state analysis (parental analysis) or initial conditions, then
2. Transient analysis

3.7. Root Zone

The impact of the lining extended to the plants, where the lining reduces or even prevents the conducting of water between the canal and the root zone or vadose zone of the agricultural land close to the canals, taking into consideration that the water level in the root zone of the plants should be maintained at specified levels to meet the needs of plants for water. Lowering the groundwater levels in the root zone due to limiting seepage from the canal did not supply plants with its requirements. Another point of view suggested that the lining process may raise the groundwater levels in the root zone by preventing percolation from the soil to the canal, which leads to the undesirable phenomenon of land logging, which hurts plants and the productivity of cultivated land. When a canal is empty due to the shift schedule between the canals network in any pilot area, as a solution for

the abundance of surface water or during periods of reduced needs, and where canals had to be maintained and therefore are not used, the seepage in the canal is also off and water levels are at a minimum. This allows seepage from agricultural land into the canal during this time, where the level of groundwater exceeds the level of water in canals; thus, the leaching line will be from the clay layer to the canal, which means that plants lose their supply of water in the root zone through periods of reduced needs. Hence, the maximum safe groundwater level for plants should be 0.75:1.50 m, as mentioned by [13], to avoid the phenomena of land logging. Thus, estimating groundwater levels in the study area before and after the concrete lining is a necessity.

3.8. Model Calibration

For model calibration, the groundwater levels calculated by SEEP/W are compared with the measured water levels. The net difference is 4 cm for the Sero canal, 1.3 cm for the Dafan canal, and 8 cm for the New-Aslogy canal. The correlation factor is 0.999, which indicates a high relation between the groundwater table computed by SEEP/W and the measured values in the field by [28].

4. Results

The results present the effect of the lining on pore water pressure (p_{wp}), especially the line of zero p_{wp}, which refers to the groundwater table. The results also present flux at a section that can reflect the influence of the lining process, such as a section at a side slope before and after the lining and the section downstream the embankment to illustrate the seepage in/out of the canal. In this study, three cases in the Nile Delta were considered in different regions to assess the impact of ICR; these included the Sero, Naw-Aslogy, and Dafan canals. SEEP/W was used to analyze the results of all the canals for three cases: unlined, lined, and lined with a drainage pipe. The results of all the cases are presented in the following sections.

4.1. Total Head and Velocity Vectors in the Steady State

An example for the results of the simulation for the selected canals is shown in Figure 5. It shows the results for the Sero canal at 1.00 km (from the inlet). Figure 5a shows the total head and velocity vectors, where the contour lines display the values of the total head in the aquitard. The total head ranged from −8 to 5.5 m. Negative values refer to negative pressure. The velocity vectors are in descending order, as velocity vectors originated from the bed of the canal, the side slope of the canal, and the vadose zone. Figure 5b represents the case of the canal after lining; the values of total heads decreased due to seepage from the canal decreasing, and where they are in a positive relation, the values of the total heads ranged from 0 to −8 m in most of the aquitard. Figure 5c shows the case of lining with drainage pipes, with the velocity vectors originating from the drainage pipe, making a spot of 6 to 8 m high heads in the aquitard. Figure 5d presents the case of an ideal lining, where there is no leakage from canal to the soil at all. It notes the aquitard in this part as an unsaturated zone, and this can be noticed from the decreased negative values of the total head, where the maximum values do not reach zero.

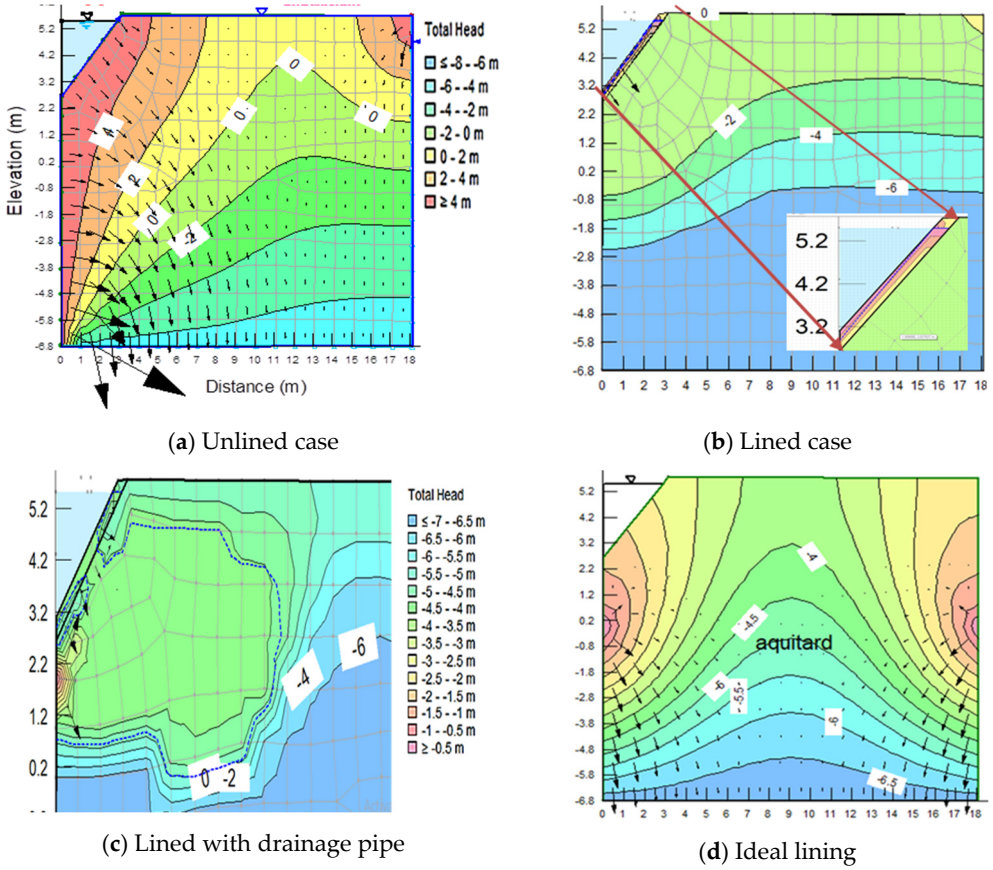

(**a**) Unlined case

(**b**) Lined case

(**c**) Lined with drainage pipe

(**d**) Ideal lining

Figure 5. Total head and velocity vectors for the Sero canal at 1.00 km for the three cases compared with the ideal case.

4.2. Pore Water Pressure at Different Sections of the Studied Canal

The p_{wp} is a good indicator for the groundwater table. The p_{wp} is determined at three sections for the Sero canal: at 1.00, 7.00, and 10.550 km. Figure 6a shows the p_{wp} for the unlined canal at the 1.00 km section. The line of zero p_{wp} separated the aquitard zone below the canal to the saturated/unsaturated, where the water pressure values are positive in the region adjacent to the canal, indicating a case of saturation and leaving the other area in the unsaturated case, where the values of p_{wp} are negative. In Figure 6b, where water was prevented from seeping due to the lining, the aquitard is a completely unsaturated zone. In Figure 6c the origination of the saturated zone was a reaction to the seepage through the drainage pipe, while the rest of the region is still in unsaturated case.

Figure 7a shows the p_{wp} for the unlined Sero canal at the section at 7.00 km. The zone is almost saturated, indicating the presence of seepage from the canal side to the soil. The values of p_{wp} at most nodes are positive. The water table reached 3.84 m at the end of the embankment. In Figure 7b, where the lining held percolation from the canal to negligible values, a remarkable shrinkage in the saturated area compared with the unlined case. The steady state status was reached after 365 days of simulation. Figure 7c shows an increasing of the area of the saturated zone as a reaction to seepage through the drainage pipe, while the rest of the region is still unsaturated. The case of the drainage pipe reached a steady state at 11 days from the start of the simulation. The seepage did not affect the land adjacent to the embankment.

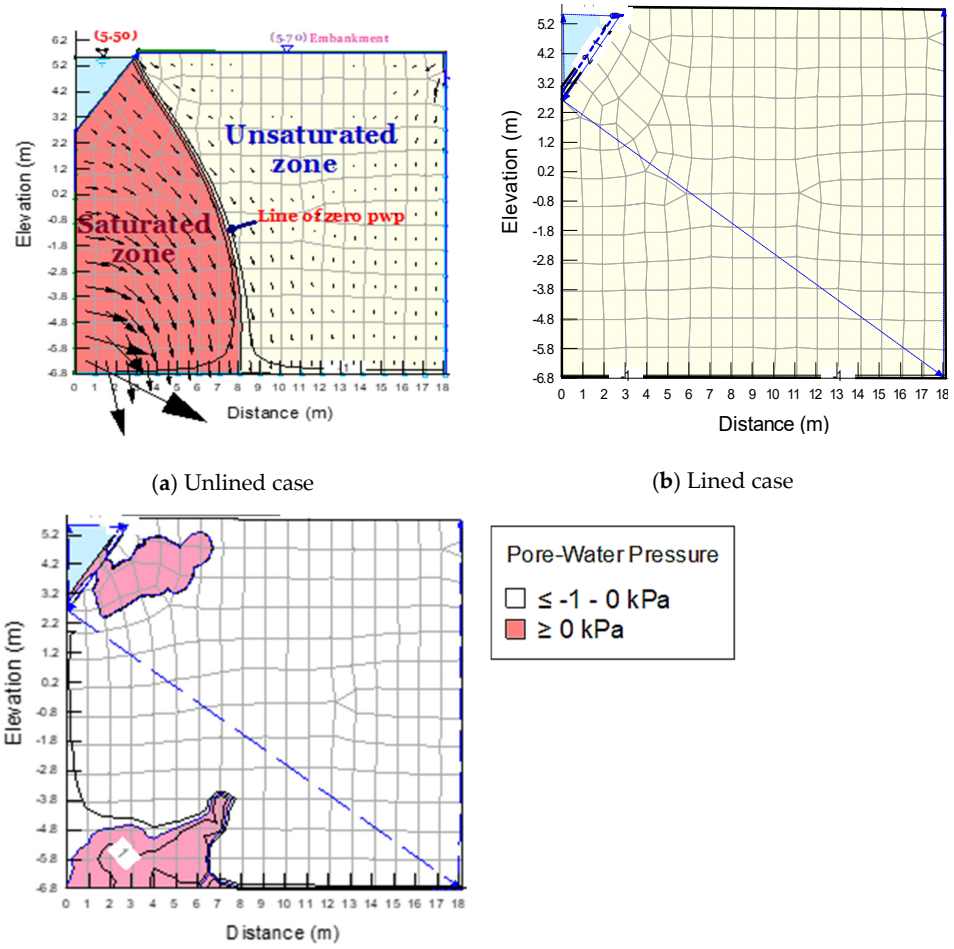

(**a**) Unlined case

(**b**) Lined case

(**c**) Lined with drainage pipe

Figure 6. p_{wp} for the Sero canal at 1.00 km.

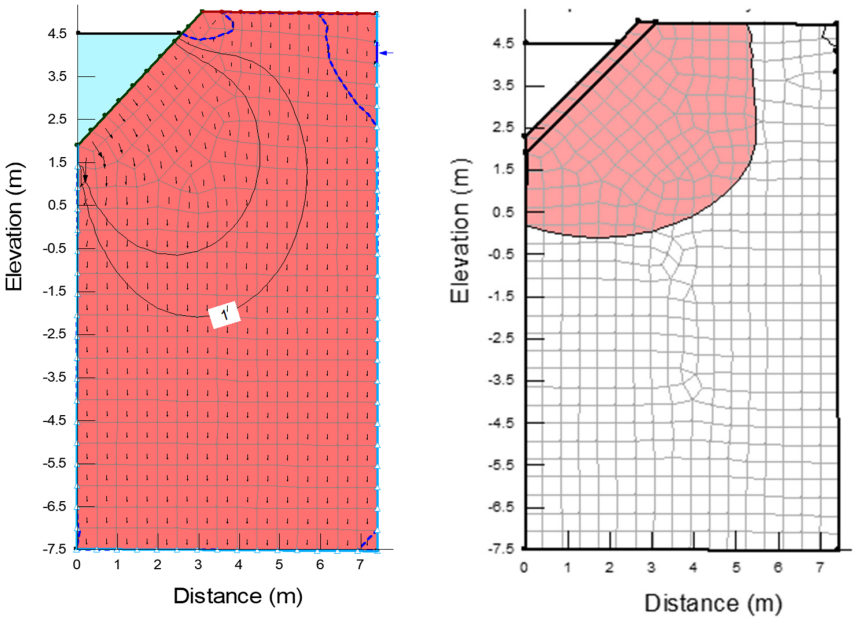

(**a**) Unlined case

(**b**) Lined case

Figure 7. *Cont.*

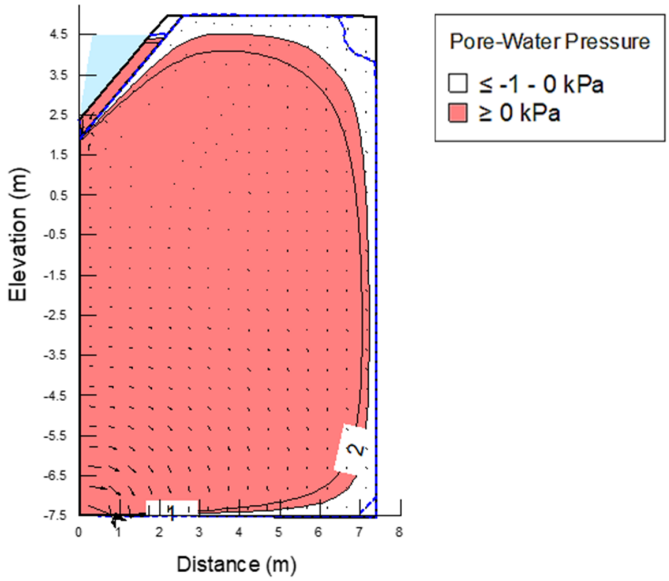

(**c**) Lined with drainage pipe

Figure 7. p_{wp} for the Sero canal at 7.00 km.

The p_{wp} for the unlined Sero canal at the section at 10.55 km is shown in Figure 8a. The zone is almost saturated, indicating the presence of seepage from the canal side to the soil. The values of p_{wp} at most nodes are positive. The water table is 3.32 m at the end of the embankment. In Figure 8b, where water is prevented from seeping due to the lining, the unsaturated zone expanded to a level near to the level of the canal bed, where the region reached a steady state 1440 days from the start of the simulation. The water table at the end of the embankment was −3.08 m. Figure 8c shows an increase in the area of the saturated zone compared to the unlined case, due to the seepage through the drainage pipe, while the rest of the region is still unsaturated. The case of the drainage pipe reached a steady state at 765 days from the start of the simulation. The water table reached −3.08 m at the end of the embankment.

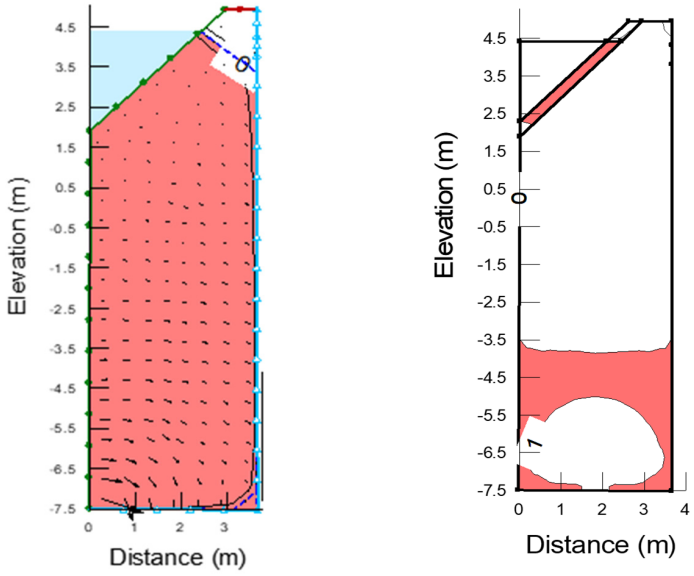

(**a**) Unlined case

(**b**) Lined case

Figure 8. *Cont.*

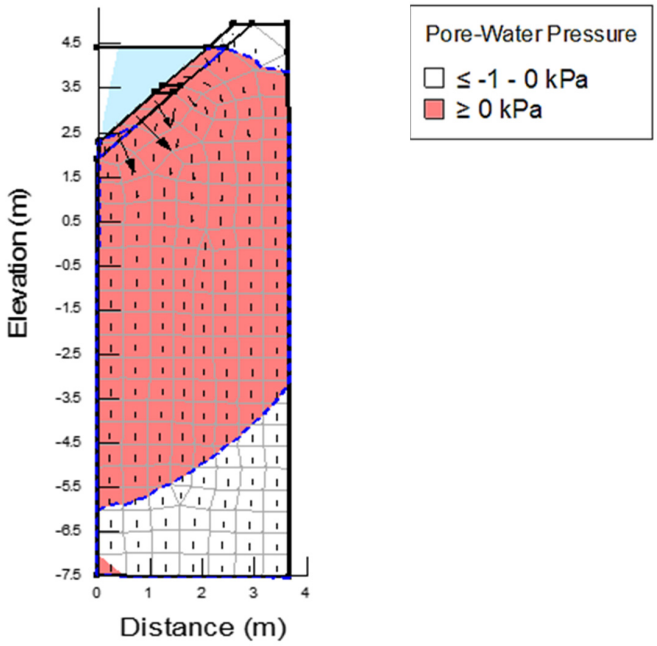

(**c**) Lined with drainage pipe

Figure 8. p_{wp} for the Sero canal at 10.55 km.

The results of p_{wp} for the Dafan canal is shown in Figure 9a–c. Figure 9a shows the p_{wp} for the unlined canal at section 17.50 km. The area of the saturated zone is more than the area of the unsaturated zone, the water table indicating the presence of seepage from the canal side to the soil, where it connected between the level of the surface water in the canal and a level of −3.05 m at the end of the embankment. The case of the unlined canal reached a steady state in a very short time. The values of p_{wp} at most nodes are positive. In Figure 9b, where seepage from the canal was nearly zero due to the lining material conductivity, the whole embankment was unsaturated, and the case of the lined canal reached a steady state at 960 days from the start of the simulation. Figure 9c shows an increase of the area of the saturated zone compared to the case of a lining, as a reaction of seepage through the drainage pipe, while the rest of the region is still unsaturated. The infiltration from the agricultural land induces a rising of the water table. The case of the lining with a drainage pipe reached a steady state at 3650 days.

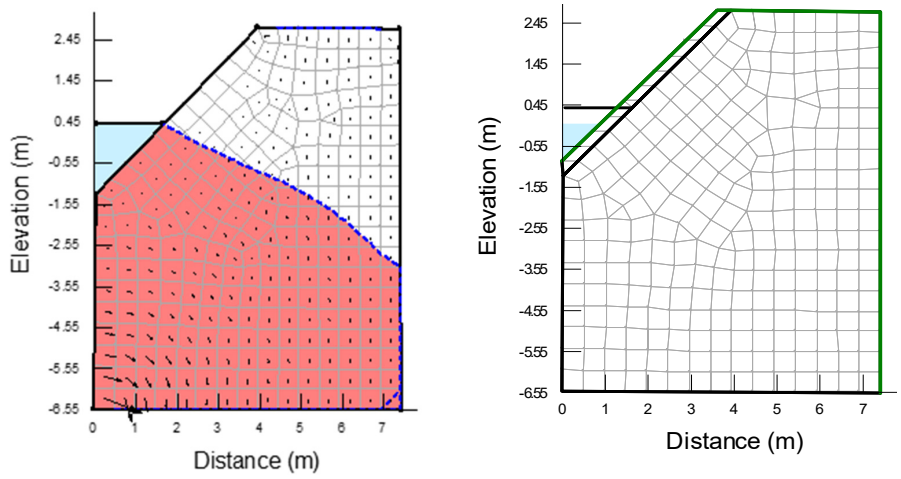

(**a**) Unlined case

(**b**) Lined case

Figure 9. *Cont.*

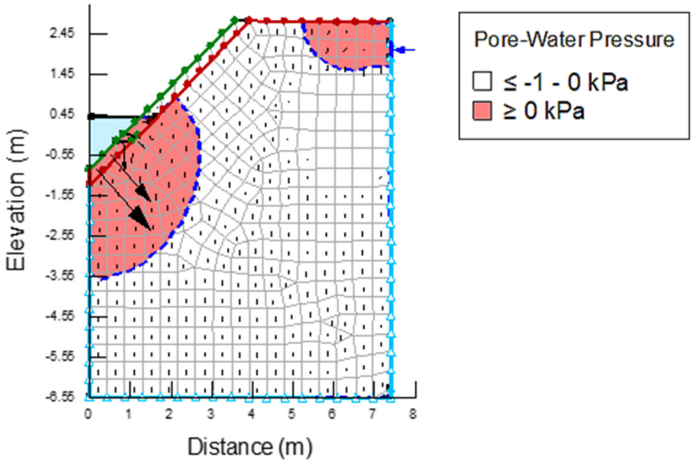

(**c**) Lined with drainage pipe

Figure 9. p_{wp} for the Dafan canal at 17.50 km.

The p_{wp} for the New-Aslogy canal is shown in Figure 10a–c. Figure 10a shows the p_{wp} for the unlined canal at section 1.500 km. The embankment area is almost saturated. The level is 8.04 m at the end of the embankment. The case of the unlined canal reached a steady state in a short time. The values of p_{wp} at most nodes are positive. In Figure 10b, where the lining prevented water from seeping, the whole embankment was unsaturated. The case of the lined canal reached a steady state at 25 days from the start of the simulation. Figure 10c shows an increase in the area of the saturated zone adjacent to the location of the drainage pipe compared to the case of lining as a reaction to seepage through the drainage pipe, while the rest of the region is still unsaturated. The case of the drainage pipe reached a steady state at 25 days from the start of the simulation. The drainage pipe did not affect the water table at the embankment.

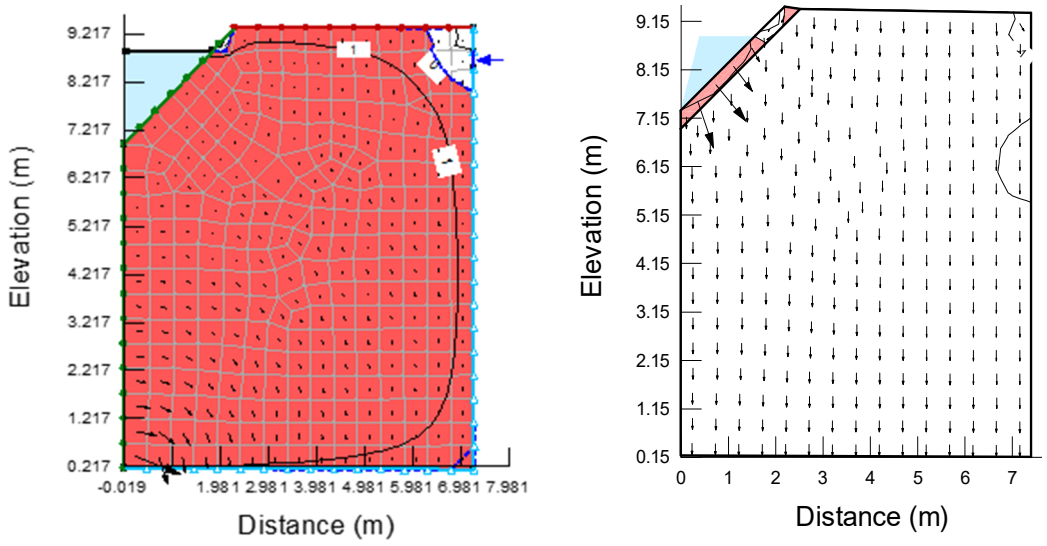

(**a**) Unlined case

(**b**) Lined case

Figure 10. *Cont.*

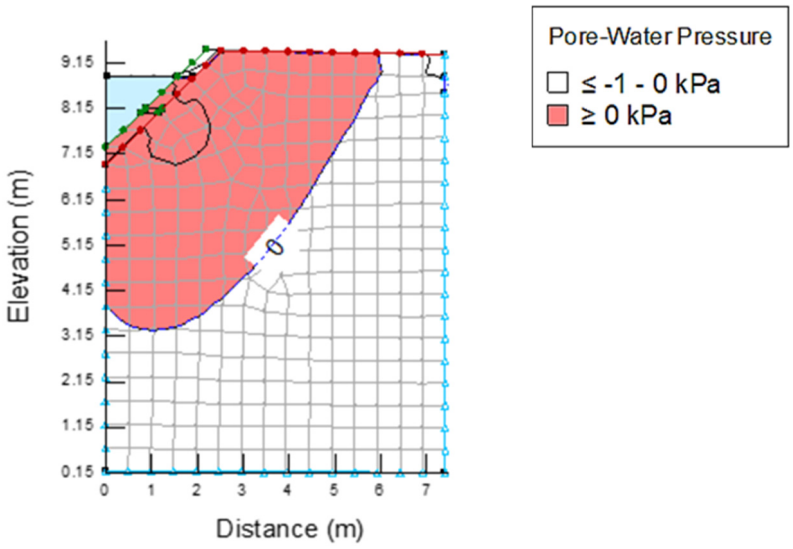

(**c**) Lined with drainage pipe

Figure 10. p_{wp} for the New-Aslogy canal at 1.50 km.

4.3. Seepage at Different Sections of the Studied Canal

The changes alerted to the seepage from canals to the aquitard and vice versa were estimated for the three cases of the canal through the drawing of flux sections. The most important sections that could clarify the changes in flux were the section at the side slope of the canal and the section downstream of the embankment. This step revealed the achieved goals of lining the canals. The flux through the lining material related to hydraulic conductivity, hydraulic gradient, and porosity, as mentioned by Darcy's Law in Equation (4):

$$v = \frac{ki}{n} \tag{4}$$

where:

1. *v:* velocity
2. *K:* hydraulic conductivity
3. *i:* hydraulic gradient
4. *n:* porosity

4.3.1. Seepage along the Side Slope for the Sero Canal at 1.00 km

The flux was fixed along the side slope with time for the unlined case. The flux was in a positive relation with the depth of the water, assessed at 0.053 m^3/day at the bed and 0.14 m^3/day at the top, where velocity distribution affects the flux values. The velocity distribution is at a maximum near the water surface and almost zero at the bed. A positive flux value referred to the direction of the flux from the canal to the soil, hence an outflow. The considered section for the lining case was the section just after the lining material. The seepage values varied along the side slope; they were negative and diminished to tiny values at the maximum height of the water: 0.00255 m^3/day and 0.0031 m^3/day. Therefore, the inflow flux was the highest near the bed and lowest near the node of the water table. The values of flux at the outlet of the drainage pipe were positive and ranged from 0.00029 to 0.00057 m^3/day. The values above or under the drainage pipe were negative, indicating seepage from the soil to the canal, where the drainage pipe created a saturation case in the embankment, allowing water to pass from the embankment to the lining material, which was less in the degree of saturation; hence, the inflow to the lining material was higher above the drainage pipe than under the drainage pipe, where the degree of saturation was higher under the drainage pipe. To evaluate the performance of the drainage pipe in saving water, a summation of fluxes for different nodes above/at/under the drainage pipe was the

indicator. The total outflow flux was 0.011 m^3/day, and the total inflow was 0.0049 m^3/day, meaning the case of the lining with a drainage pipe was classified as outflow and estimated to be 0.0059 m^3/day.

4.3.2. Seepage along the Side Slope for the Sero Canal at 7.00 km

The flux was positive at the side slope for the unlined case, indicating the seepage direction from the canal to the aquitard. The flux was related to the depth of the water and assessed at 0.0353 and 0.0027 m^3/day for the bed and top of the canal, respectively. The relationship between the flux and the depth along the section just after the lining material was negative and ranged from 0.077 m^3/day at the bed of the canal to 0.001 m^3/day near the water table. The flux above the drainage pipe was zero, 9.94×10^{-8}, -1.14 m^3/day. The negative flux refers to inflow to the lining layer due to seepage from the root zone, which is an impact in this case of the small bank width. The lower limit of the drainage pipe was outflow and was 1.35×10^{-6} m^3/day. The part of the side slope under the drainage pipe was exposed to inflow in its upper part due to the saturation state created by the drainage pipe, which allowed water to move to the less saturated layer of the lining material; the flux was -0.044 m^3/day, and by moving downwards the state of saturation disappeared, which allowed the layer of the lining material to show small values of flux according to its permeability, which was 1.35×10^{-6} m^3/day after 11 days of simulation. The net flow was inflow and measured at -0.044 m^3/day, wherever the small bank width allowed seepage originating from the root zone to modify the flow movement.

4.3.3. Seepage along the Side Slope for the Sero Canal at 10.55 km

The flux at the side slope for the unlined case was positive, indicating the ordinary seepage direction from the canal to the aquitard. The flux increased downwards and was estimated at 0.046 and 0.007 m^3/day for the top and the bed of the canal, respectively, while the flux for the lining case was inflow and measured -0.062 m^3/day at the bed of the canal, influenced by infiltration from the root zone, which had a more discernible affect than the prior sections due to the small bank width. The flux value faded to zero near the water table. The flux over the drainage pipe was outflow just above the upper boundary of the drainage pipe and evaluated at 0.016 m^3/day. The effect of the near root zone inverted the flux to inflow near the water table. Figure 7c explains the saturation of this part of the lining material. The inflow was estimated at -0.0015 m^3/day. The flux for the lower/upper boundaries of the drainage pipe was outflow and estimated at 0.023/0.016 m^3/day, where the drainage pipe was located, aside from the influence of the root zone infiltration. The part of the side slope under the drainage pipe was exposed to inflow because of the presence of the drainage pipe, which allowed water to move to the less saturated layer of the lining material. When moving downwards, the state of saturation of the lining layer disappeared, which allowed this layer smaller values of flux according to its permeability, which was -0.14 m^3/day as the net flow.

4.3.4. Seepage along the Side Slope for the Dafan Canal at 17.50 km

The flux was outflow at the side slope for the unlined case, and it was in reverse proportion to the depth. The negative values of the flux indicated seepage from the aquitard to the canal in the part above the level of 0.45 m, which was the water level in the canal. The flux at the bed node was 0.003 m^3/day, while it was 0.005 m^3/day for the node at the water table level and converted to inflow estimated at -0.006 m^3/day at the upper node of the side slope. The flux downstream from the lining material was inflow at all nodes, indicating small seepage from the aquitard to the canal, excluding three nodes at the top of the side slope where the infiltration from the vadose zone induced a small seepage into the canal, and the values of flux ranged from -0.009 m^3/day to zero near the node at the water table level. The flux over the drainage pipe was outflow; the degree of saturation and the small permeability of the lining material released water to flow out from the canal. The summation of flux for different nodes was 0.066 m^3/day. The values of flux

were outflow for the upper and lower boundaries of the drainage pipe and were 0.010 and 0.014 m^3/day. The part of the side slope under the drainage pipe was exposed to inflow due to the saturation case created by the above drainage pipe. The values of flux ranged between −0.01 m^3/day for the node just under the drainage pipe and fell to zero for the lower node on the side slope; hence the flow was outflow and estimated at −0.121 m^3/day.

4.3.5. Seepage along the Side Slope for the New-Aslogy Canal at 1.50 km

The flux at the side slope for the unlined case was outflow and in reverse proportion to the depth. There was a small inflow for the part above the level of 8.84 m, which was the water level in the canal. The outflow started from 0.004 m^3/day and ended at zero near the bed. The inflow through the side slope above the water table was −0.01 m^3/day. The flux was inflow at all nodes for the case of lining, indicating a small discharge from the aquitard to the canal, with values from −0.04 m^3/day to zero near the water table. The flux was positive for the nodes of the lower and upper limit of the drainage pipe, which means that the seepage was from the drainage pipe to the aquitard with a maximum value of 0.0181 m^3/day and 0.0117 m^3/day. The flow was inflow for above and under the drainage pipe.

4.4. Seepage along the Downstream of the Embankment at Different Sections of the Studied Canal

This section illustrates the seepage from different sections of the studied canal downstream of the embankment. Figure 11 represents the values of flux at the toe downstream of the embankment for different cases of the Sero canal at the section 1.00 km. For the unlined case, Figure 11a shows that the cumulative flux increased with time and reached 2.65 m^3 after 10 days of simulation; the positive values expressed seepage from the embankment to the irrigated land in the form of outflow. Figure 11b shows no flux across the embankment for the lined case, where the values of the cumulative flux were nearly zero for all time periods, which means there was no seepage through the downstream of the embankment. Figure 11c represents the case of a lined canal with a drainage pipe, where the cumulative flux decreased with time to 0.00087 m^3 after 10 days of simulation; the negative values expressed the flux entrance to the embankment from the adjacent soil, which referred to an increase in the degree of unsaturation of the embankment with time despite the presence of the drainage pipe, which was considered a source point, as the steady state condition was reached after 250 days.

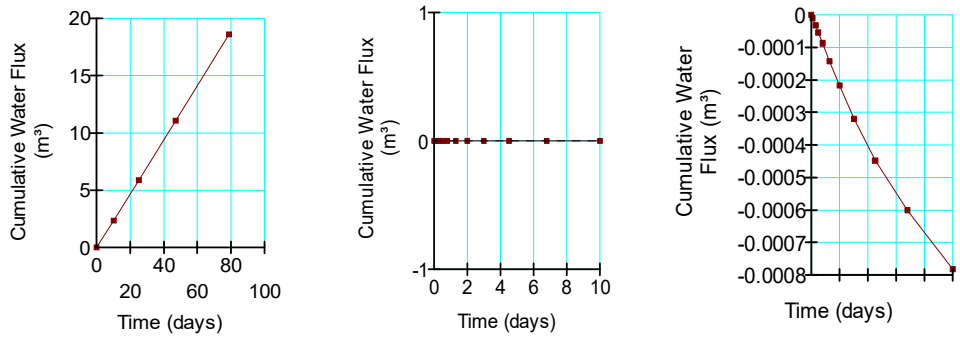

(**a**) Unlined case (**b**) Lined case (**c**) Lined drainage pipe case

Figure 11. Cumulative flux against time at the toe of the embankment at 1.00 km of the Sero canal.

The flux at the downstream of the embankment for different cases of the Sero canal at section 7.00 km is shown in Figure 12. Figure 12a shows flux values of either zero or negative. It also illustrates that the cumulative flux was proportional to time, the results indicated by Figure 12a proved that the embankment was fully saturated, hence the adjacent soil of the aquitard was also saturated; thus, the interaction between the surface water in the canal and the groundwater in the adjacent land was weak, where the maximum inflow to the embankment was 0.55 m^3 at 100 days of the simulation. This interaction was in the form of inflow to the embankment, as the negative values cleared. Figure 12b indicates

an increase in the inflow to the embankment compared to the unlined case, where the maximum inflow reached 0.578 m^3 at 100 days of the simulation, due to the presence of the lining material, which reduced infiltration from the canal, thus reducing the degree of saturation of the embankment. Figure 12c shows the lined canal with a drainage pipe and shows the importance of the drainage pipe in releasing water pressure on the side slope by allowing the inflow to the embankment then to the canal. The amount of inflow increased to 0.579 m^3 at 100 days of the simulation compared to the other two cases.

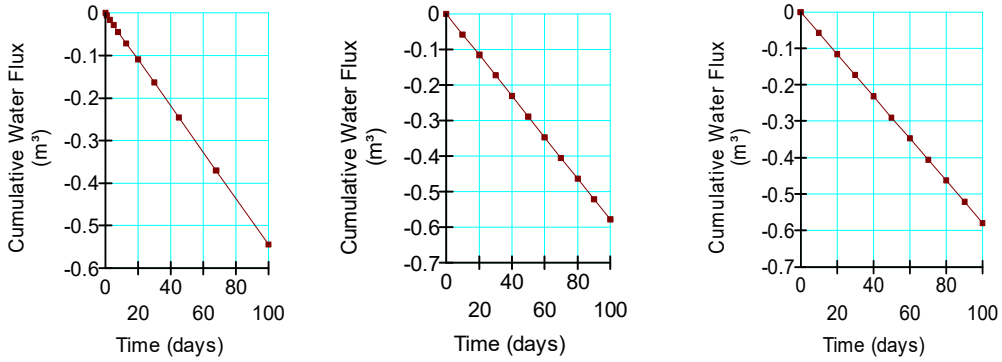

(**a**) Unlined case (**b**) Lined case (**c**) Lined with drainage pipe

Figure 12. Cumulative flux against depth across the embankment at 7.00 km of the Sero canal.

The flux downstream of the toe of the embankment for the different cases of the Sero canal at the section of 10.55 km is presented in Figure 13. Figure 13a shows the case of the unlined canal and shows that the values of cumulative flux were in a linear relation with time, which reached 0.8 m^3 for 100 days of simulation. In Figure 8a the embankment, as well as the adjacent soil, is fully saturated, so the seepage was in the form of inflow and was either zero or negative values. Zero refers to there being no movement through the aquitard due to saturation, while negative values indicate that the movement was from the irrigated soil to the embankment, which proves that the irrigated soil is more saturated than the embankment. In Figure 13b, the cumulative flux increased with time and reached 0.248 m^3 at 100 days of simulation, indicating inflow from the irrigated soil, and the results illustrated by Figure 8b show that the embankment was unsaturated, which induced the movement of flow towards the embankment. Figure 13c shows the cumulative flux for the lined canal with a drainage pipe that was proportional to time and evaluated by 0.363 m^3 at 100 days of simulation.

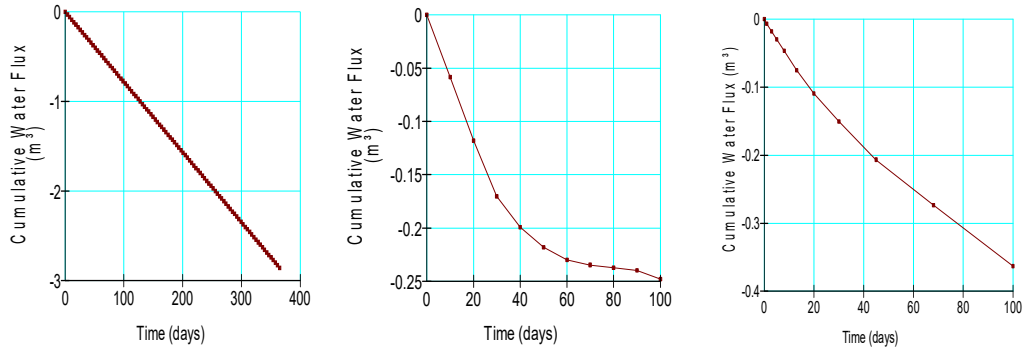

(**a**) Unlined case (**b**) Lined case (**c**) Lined with drainage pipe

Figure 13. Cumulative flux against time at the toe of the embankment at 10.55 km of the Sero canal versus time.

Figure 14 represents the values of cumulative flux at the toe of the embankment for different cases of the Dafan canal at section 17.00 km. Figure 14a represents the cumulative

flux for the unlined case. It shows negative values of flux to the embankment from the aquitard for the case of the unlined canal, as the negative values indicated and reached 0.553 m^3 at 100 days of simulation. In Figure 14b, the cumulative flux is proportional to time and was also in the form of inflow due to the infiltration from agricultural land to the embankment. The results show that the aquitard was more saturated than the embankment, where the lining reduced seepage to the embankment from the canal; hence, it reduced the degree of saturation of the embankment to 0.51 m^3 at 100 days of simulation. Figure 14c shows the cumulative flux for the lined canal with drainage that was 0.542 m^3 at 100 days of simulation and was in the form of inflow from the aquitard to the embankment.

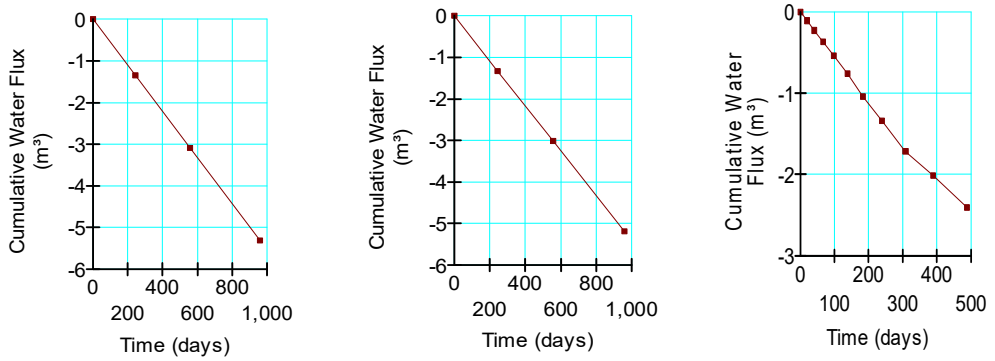

(**a**) Unlined case (**b**) Lined case (**c**) Lined with drainage pipe

Figure 14. Cumulative flux against time at the toe of the embankment at 17.00 km of the Dafan canal.

The values of cumulative flux at the toe of the downstream embankment for different cases of the New-Aslogy canal at section 1.50 km are shown in Figure 15. The cumulative flux was in a linear relation with time and represented inflow from the aquitard to the embankment for the three cases. Figure 15a shows the results of cumulative flux for the unlined case, which reached 0.531 m^3 at 100 days of simulation. This illustrates that the irrigated land was more saturated than the embankment, so the movement was from the aquitard to the embankment. Figure 15b represents the values of cumulative flux for the unlined case, where the flux was 0.495 m^3 for 100 days of simulation. Figure 15c shows the cumulative flux for the case of the lined canal with a drainage pipe. The flux value was 0.497 m^3 for 100 days of simulation. For the two cases of lining, the results in Figure 10a,b show that the embankments were unsaturated due to the lining, which induced the movement of seepage to the embankment.

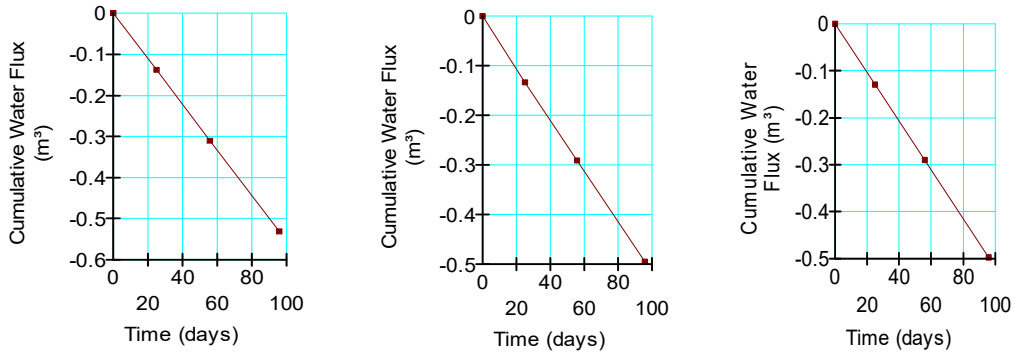

(**a**) Unlined case (**b**) Lined case (**c**) Lined drainage pipe case

Figure 15. Cumulative flux against time at the toe of the embankment at 1.50 km of the New-Aslogy canal versus time.

4.5. The Effect of the Lining on the Root Zone

The water table for the vadose zone of plants was measured for the three proposed cases at different reaches, as shown in Table 3. The water table for the case of unlined canals had the highest water level, followed by the case of lined with a drainage pipe, then the unlined case. Figure 16 shows the groundwater table for the studied cases. Most cases had a water table less than the needed moisture in the root zone, excluding the cases of unlined and lined with a drainage pipe for the Sero canal at the 7.00 km section, and the case of the unlined New-Aslogy canal [13]. This was an indicator of a shortage in the water supply.

The results showed that the seepage from the side slopes of the canals to the embankments and the infiltration from the root zone did not affect each other for all studied cases, excluding the case of lining with a drainage pipe of the Dafan canal at 17.50 km. This was due to the new policies in managing water resources, where water glutton crops became restricted, and also the modification of irrigation techniques, which depend on a smart type of irrigation that could consume the least amount of water, hence the infiltration being converted to minimum values.

Table 3. The computed groundwater table in the vadose zone.

Canal	Reach (km)	Unlined	Lined	Lined with a Drainage Pipe
Sero	1.00	1.9	1.7	1.725
	7.00	3.84	1.966	3.49
	10.550	2.4	−3.78	2.35
Dafan	1.50	−0.75	−1.03	−0.87
New-Aslogy	17.00	5.94	2.22	4.45

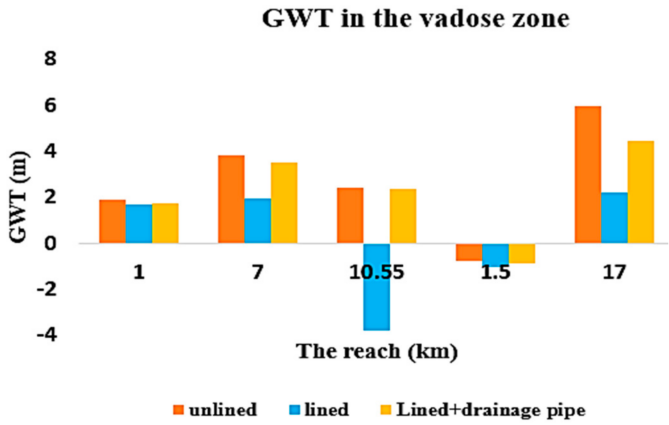

Figure 16. Groundwater table at different sections for the studied canals.

4.6. The Effect of the Embankment Width

Figures 7a, 8a, 9a, 10a and 11a showed almost saturated embankment for the unlined cases, while the cases of lining expressed an unsaturated embankment except the cases of the Sero canal at 7.00 km and 10.550 km. In the case of 7.00 km the saturated zone was nearby the side slope, where in the case of 10.550, the saturation was in the lower part of the embankment, where the width of the embankment was 7.4 m and 4.9 m for the case of 7.00 km and the case of 10.550 km, respectively. The seepage tended to settle in lower parts under gravity than travel in a longer path. For the cases of lining with a drainage pipe, the saturation zone was nearby the side slope due to the small seepage through the lining material. Figures 9c and 10c showed that the saturation zone extended from the side slope to the end of the embankment, where these two cases have the smallest bank width. The bank widths are 4.9 m and 5.5 m respectively.

5. Conclusions

Irrigation canal rehabilitation (ICR) is considered a good solution to save surface water through lining the canal bed and sides with impermeable materials. This is particularly important for countries suffering from water shortages, such as Egypt. ICR is a great national project for the management of surface water in Egypt. This paper evaluated the effect of ICR in preventing losses from canals to the groundwater aquitard and even to the nearby land through the leaching line. The results at the side slope showed that the ICR achieved the targeted goals upon comparing the flux for the cases of unlined, lined, and lined with a drainage pipe, where the highest flux came from the unlined case, followed by the case of lined with a drainage pipe, while the lined case reaches were not far from preventing seepage from the canal, where any lining material as well as the applied and examined lining material in the present work has permeability.

The infiltration from canals had no perceptible influence on seepage from agricultural land to the embankment of the canal as well as p_{wp}, velocity vectors, and the total heads excluding one case. The width of the bank affected the case of saturation/unsaturation, where the long path allows water to seep downward rather than moving towards agricultural land. Thus, it tended to make the embankment more unsaturated than saturated. So, there was a relation between the width of the bank and its degree of saturation. This relation was recommended for further separate study. The vadose zone is affected by lowering the groundwater table in most cases, but because of applying new untraditional ways of irrigation, such as sprinkler and drip irrigation, this effect could disappear.

The results for the effect of a lining on the embankment proved that the lining was a helpful solution to minimize the seepage from canals to the embankment, while seepage through the toe of the embankment was affected by the lining. The water table in the vadose zone was less than the upper and lower limits. The remarkable lowering in the GWT converted the embankment to an unsaturated zone at lined reaches, while at lined reaches with drainage pipes, the drainage pipe acted as a source point and seeped water to the embankment and restored the unsaturated state for only the upper part of the embankment. The ICR helped in reducing the conductance between the embankment and the adjacent lands by 75% and reached 100% in three cases from fifteen studied cases. The average reduction was 94.39% for lined reaches and 91.09% for lined reaches with drainage pipes. Matching results with El-Molla [31] mentioned that compacted earth lining could reduce seepage by 99.8%. Han et al. [17] proved that the combination concrete and geomembrane lining reduced seepage by 86%; the efficiency of the lining process could be developed by employing certified techniques to protect extra lost water.

The new applied policy of smart irrigation links the measurements of moisture in the vadose zone with smart phones to urge users to use the most suitable time and amount of irrigation.

Author Contributions: Conceptualization, H.F.A.-E. and S.A.-E.; methodology, S.A.-E. and H.F.A.-E.; software, S.A.-E.; validation, M.Z., S.A.-E., B.K. and H.F.A.-E.; formal analysis, H.F.A.-E.; investigation, H.F.A.-E.; resources, M.Z. and B.K.; data curation, H.F.A.-E. writing—original draft preparation, S.A.-E.; writing—review and editing, B.K. and H.F.A.-E.; visualization, M.Z.; supervision, H.F.A.-E.; project administration, H.F.A.-E.; funding acquisition, M.Z. All authors have read and agreed to the published version of the manuscript.

Funding: This research received no external funding.

Data Availability Statement: The data are not publicly available due to institutional property rights.

Acknowledgments: This work was supported by the Slovak Research and Development Agency under the Contract no. APVV-20-0281, and a project funded by the Ministry of Education of the Slovak Republic VEGA1/0308/20 "Mitigation of hydrological hazards, floods, and droughts by exploring extreme hydroclimatic phenomena in river basins".

Conflicts of Interest: The authors declare no conflict of interest.

References

1. Zeng, N.; Cen, L.; Xie, Y.; Zhang, S. Nonlinear optimal control of cascaded irrigation canals with conservation law PDEs. *Control Eng. Pract.* **2020**, *100*, 104407. [CrossRef]
2. Rath, A.; Swain, P.C. Evaluation of performance of irrigation canals using benchmarking techniques—A case study of Hirakud dam canal system, Odisha, India. *ISH J. Hydraul. Eng.* **2020**, *26*, 51–58. [CrossRef]
3. Zhou, X.; Zhang, Y.; Sheng, Z.; Manevski, K.; Andersen, M.N.; Han, S.; Li, H.; Yang, Y. Did water-saving irrigation protect water resources over the past 40 years? *A global analysis based on water accounting framework. Agric. Water Manag.* **2021**, *249*, 106793. [CrossRef]
4. Khanal, K.; Adhikari, K.B.; Dhakal, S.C.; Marahatta, S. Factors Motivating Farmers for Collective Action for Management of Irrigation System in Nepal. *Int. J. Soc. Sci. Manag.* **2021**, *8*, 285–291. [CrossRef]
5. Morad, N.A.; Abdel Latif, R.M. Assessment of Surface Water-Groundwater Relationship in the Area between Borg El Arab and West El Hammam, North West Coastal Zone, Egypt. *Bull. Fac. Eng. Mansoura Univ.* **2020**, *42*, 1–11. [CrossRef]
6. Awad, S.R.; El Fakharany, Z.M. Mitigation of waterlogging problem in El-Salhiya area, Egypt. *Water Sci.* **2020**, *34*, 1–12. [CrossRef]
7. Rank, P.; Vishnu, B. Pulse drip irrigation: A review. *J. Pharmacogn. Phytochem.* **2021**, *10*, 125–130.
8. Hosseinzadeh Asl, R.; Salmasi, F.; Arvanaghi, H. Numerical investigation on geometric configurations affecting seepage from unlined earthen channels and the comparison with field measurements. *Eng. Appl. Comput. Fluid Mech.* **2020**, *14*, 236–253. [CrossRef]
9. Tavakoli, E.; Ghorbani, B.; Radfar, M.; Borujeni, H.S.; Ghahraman, B. Investigating the Impressibility of Groundwater Level from Infiltration and Seepage in Water Conveyance Channels (Case Study: Boldaji). *Irrig. Sci. Eng.* **2020**, *42*, 1–14.
10. Deng, C.; Bailey, R.T. Assessing causes and identifying solutions for high groundwater levels in a highly managed irrigated region. *Agric. Water Manag.* **2020**, *240*, 106329. [CrossRef]
11. Habteyes, B.G.; Ward, F.A. Economics of irrigation water conservation: Dynamic optimization for consumption and investment. *J. Environ. Manag.* **2020**, *258*, 110040. [CrossRef]
12. Souza, G.; Aquino, P.T.; Maia, R.F.; Kamienski, C.; Soininen, J.-P. A fuzzy irrigation control system. In Proceedings of the 2020 IEEE Global Humanitarian Technology Conference (GHTC), Seattle, WA, USA, 29 October–1 November 2020. [CrossRef]
13. Aziz, S.A.; Negm, A.; Abd-Elhamid, H.F.; Mustafa, G.; Nassar, M. The impact of irrigation canals covering on groundwater in the nile delta, a case study: Abu Kebier city, Sharkia, Egypt. *Int. Water Technol. J.* **2009**, *5*, 57–64.
14. Nasr, R.; Zeydan, B.; Bakry, M.; Saloom, M. Uplift pressure relief on lined canals using tile drains. *Alex. Eng. J.* **2003**, *42*, 497–507.
15. Abuzeid, T.S. Conveyance losses estimation for open channels in middle Egypt case study: Almanna main canal, and its branches. *JES J. Eng. Sci.* **2021**, *49*, 64–84. [CrossRef]
16. Shah, Z.; Gabriel, H.; Haider, S.; Jafri, T. Analysis of seepage loss from concrete lined irrigation canals in Punjab, Pakistan. *Irrig. Drain.* **2020**, *69*, 668–681. [CrossRef]
17. Han, X.; Wang, X.; Zhu, Y.; Huang, J.; Yang, L.; Chang, Z.; Fu, F. An Experimental Study on Concrete and Geomembrane Lining Effects on Canal Seepage in Arid Agricultural Areas. *Water* **2020**, *12*, 2343. [CrossRef]
18. Eltarabily, M.G.; Moghazy, H.E.; Abdel-Fattah, S.; Negm, A.M. The use of numerical modeling to optimize the construction of lined sections for a regionally-significant irrigation canal in Egypt. *Environ. Earth Sci.* **2020**, *79*, 80. [CrossRef]
19. Abd-Elhamid, H.F.; Abdelaal, G.M.; Abd-Elaty, I.; Said, A.M. Efficiency of using different lining materials to protect groundwater from leakage of polluted streams. *J. Water Supply Res. Technol.* **2019**, *68*, 448–459. [CrossRef]
20. Khan, M.H.A.; Saleem, M.U.; Ahmad, S.R.; Ahmad, N.; Sameeni, S.J.; Akram, M.; Farooq, M. Role of Canal Lining on Groundwater Fluctuations: A Modeling Simulation Approach for Jaalwala Distributary, Bahawalnagar. *Open J. Appl. Sci.* **2017**, *7*, 213–232. [CrossRef]
21. Lesser, L.E.; Mahlknecht, J.; López-Pérez, M. Long-term hydrodynamic effects of the All-American Canal lining in an arid transboundary multilayer aquifer: Mexicali Valley in north-western Mexico. *Environ. Earth Sci.* **2019**, *78*, 504. [CrossRef]
22. Zhao, Y.; Li, F.; Yao, R.; Jiao, W.; Hill, R.L. An Empirical Orthogonal Function-Based Approach for Spatially- and Temporally-Extensive Soil Moisture Data Combination. *Water* **2020**, *12*, 2919. [CrossRef]
23. Taran, F.; Mahtabi, G. Optimum layout of weep holes in concrete irrigation canals to control uplift pressure and hydraulic gradient. *Arab. J. Geosci.* **2020**, *13*, 88. [CrossRef]
24. Salmasi, F.; Khatibi, R.; Nourani, B. Investigating reduction of uplift forces by longitudinal drains with underlined canals. *ISH J. Hydraul. Eng.* **2017**, *24*, 81–91. [CrossRef]
25. Abd-Elaziz, S.; Zeleňáková, M.; Mésároš, P.; Purcz, P.; Abd-Elhamid, H.F. Anthropogenic Activity Effects on Canals Morphology, Case Study: Nile Delta, Egypt. *Water* **2020**, *12*, 3184. [CrossRef]
26. Aziz, S.A.; Zeleňáková, M.; Mésároš, P.; Purcz, P.; Abd-Elhamid, H. Assessing the Potential Impacts of the Grand Ethiopian Renaissance Dam on Water Resources and Soil Salinity in the Nile Delta, Egypt. *Sustainability* **2019**, *11*, 7050. [CrossRef]
27. Available online: https://geoportal.mwri.gov.eg/portal/apps/webappviewer/index.html?id=81955815d2a84d1890b4d3686dc6be8a (accessed on 20 March 2021).
28. Engineering tooLfC. *Soil Sampling*; Technical Report; Engineering tooLfC: Zagazig, Egypt, 2019.
29. Division of Agricultural Sciences and Natural Resources Hsoe. Available online: https://www.osuit.edu/ (accessed on 20 April 2021).

30. Chuck Burr UoN-L. *PAGE 3, Irrigation Chapter 3—Soil Water*; The Plant and Soil Sciences eLibrary: Lincoln, NE, USA, 2021; Available online: https://passel2-stage.unl.edu/view/lesson/bda727eb8a5a/3, (accessed on 25 May 2021).
31. El-Molla, D.A.; El-Molla, M.A. Reducing the conveyance losses in trapezoidal canals using compacted earth lining. *Ain Shams Eng. J.* **2021**, *12*, 2453–2463. [CrossRef]
32. Aghdam, A.T.; Salmasi, F.; Abraham, J.; Arvanaghi, H. Effect of Drain Pipes on Uplift Force and Exit Hydraulic Gradient and the Design of Gravity Dams Using the Finite Element Method. *Geotech. Geol. Eng.* **2021**, *39*, 3383–3399. [CrossRef]
33. Salmasi, F.; Abraham, J. Predicting seepage from unlined earthen channels using the finite element method and multi variable nonlinear regression. *Agric. Water Manag.* **2020**, *234*, 106148. [CrossRef]
34. Jassam, M.G.; Abdulrazzaq, S.S.; Khalaf, W.D. Seepage characteristics analysis through homogeneous earth dams using theoretical model of SEEP/W program. *J. Crit. Rev.* **2020**, *7*, 5984–5996.
35. Al-Janabi, A.M.S.; Ghazali, A.H.; Ghazaw, Y.M.; Afan, H.A.; Al-Ansari, N.; Yaseen, Z.M. Experimental and Numerical Analysis for Earth-Fill Dam Seepage. *Sustainability* **2020**, *12*, 2490. [CrossRef]
36. Al-Nedawi, N.M. Finite Element Analysis of Seepage for Hemrin Earth Dam Using Geo-Studio Software. *Diyala J. Eng. Sci.* **2020**, *13*, 66–76. [CrossRef]
37. Mostafa, A.; Gado, T.A.; Masoud, A.A.; Rashwan, I.M.H. Numerical and experimental analyses of the use of double vertical barrier walls for groundwater protection. *Water Environ. Res.* **2020**, *92*, 2168–2177. [CrossRef] [PubMed]
38. Geo-Studio. *Version 8.15.11236 UMGI, Calgary, in, Alberta, Canada*; Geo-Studio: Calgary, AB, Canada, 2012.
39. (WGNHS) TWGaNHS. *Understanding Porosity and Density*; (WGNHS) TWGaNHS: Hong Kong, China, 2021.